Molecular Pharmacology Fast Forward. Published on September 24, 2018 as DOI: 10.1124/mol.118.113399
This article has not been copyedited and formatted. The final version may differ from this version.

Betacellulin (BTC) Biases the EGFR to Dimerize with ErbB3

Jamie S. Rush, Joanne L. Peterson, Brian P. Ceresa

Department of Pharmacology and Toxicology (J.S.R., J.L.P, B.P.C.) and
Department of Visual Science (B.P.C), University of Louisville, Louisville, KY
40202,

Molecular Pharmacology Fast Forward. Published on September 24, 2018 as DOI: 10.1124/mol.118.113399
This article has not been copyedited and formatted. The final version may differ from this version.

Running title: BTC promotes EGFR:ErbB3 heterodimers

To whom correspondence should be addressed: Brian P. Ceresa, CTRB Rm 305, 505 S. Hancock St., Louisville, KY 40202. brian.ceresa@louisville.edu

Number of text pages: 31
Number of tables: 0
Number of Figures: 6
Number of Supplemental Figures: 1
Number of References: 60
Number of words in Abstract: 210
Number of words in Introduction: 866
Number of words in Discussion: 1095

Abbreviations: Bovine Serum Albumin (BSA); Betacellulin (BTC); Epidermal Growth Factor (EGF); Epidermal Growth Factor Receptor (EGFR); Immunoblot (IB); Immunoprecipitation (IP); ErbB3 antagonist/seribantumab (MM-121); neuregulin 4 (NRG4); polyacrylamide gel electrophoresis (PAGE)supernatant from an immunoprecipitation/pass through (PT); receptor tyrosine kinase (RTK); sodium dodecyl sulfate (SDS);

Abstract:

There are thirteen known endogenous ligands for the Epidermal Growth Factor Receptor (EGFR) and its closely related ErbB receptor family members. We previously reported that Betacellulin (BTC) is more efficacious than Epidermal Growth Factor (EGF) in mediating corneal wound healing [Peterson et al. (2014) IOVS 55(5):2870-80], although the molecular basis for this difference was unknown. For the most part, differences between ligands can be attributed to variability in binding properties, such as each ligand's unique rate of association and dissociation, pH sensitivity, and selective binding to individual ErbB family members. However, this was not the case for BTC. Despite being better at promoting wound healing via enhanced cell migration, BTC has reduced receptor affinity and weaker induction of EGFR phosphorylation. These data indicate that BTC's response is not due to enhanced affinity or kinase activity. Receptor phosphorylation and proximity ligation assays indicate that BTC treatment significantly increases ErbB3 phosphorylation and EGFR:ErbB3 heterodimers when compared to EGF treatment. We observed EGFR:ErbB3 heterodimers contribute to cell migration, as the addition of an ErbB3 antagonist (MM-121) or RNAi-mediated knockdown of ErbB3 attenuates BTC-stimulated cell migration as compared to EGF. Thus, we demonstrate that despite both ligands binding to the EGFR, BTC biases the EGFR to dimerize with ErbB3 to regulate the biological response.

Molecular Pharmacology Fast Forward. Published on September 24, 2018 as DOI: 10.1124/mol.118.113399
This article has not been copyedited and formatted. The final version may differ from this version.

Introduction:

The ErbB family of receptor tyrosine kinases (RTKs) have well-established roles in developmental biology, tissue homeostasis, and cancer biology (Chen et al., 2016; Wieduwilt and Moasser, 2008). All four family members [ErbB1 (Epidermal Growth Factor Receptor-EGFR), ErbB2, ErbB3, and ErbB4] share a number of structural and functional features including their size, transmembrane orientation of the protein, and mechanism of activation. Activation of ErbB receptors begins with ligand binding that induces receptor dimerization, transphosphorylation of cytoplasmic tyrosines, and docking of downstream effectors to those phosphotyrosines. These activated effectors induce biochemical changes that lead to modifications in cell biology. Each ErbB family member is unique in its activating ligands, degree of kinase activity, and cadre of downstream effectors. These features confer receptor-specific biochemical signals, which regulate the resulting cell biology.

Receptor specific ligands initiate ErbB RTK signaling. There are 13 known ligands for the ErbB family of proteins, each encoded by a distinct gene (Pathak et al., 1995). These ligands differ in their tissue distribution as well as their rates of association and dissociation to each receptor. Not only do ligands drive the specificity of receptor:effector interactions, but also the duration and magnitude of effector response through differences in membrane trafficking (Wang and Hung, 2012; Wiley, 2003). Ultimately, the ligand specific mechanisms influence the cellular and physiological responses.

Despite the appreciation that ligands can induce receptor-specific signaling events, the molecular basis for these differences are not always clear due to the intrinsic barriers to ligand analysis. Knockdown of the EGFR results in embryonic lethality in mice, or death shortly after birth, highlighting its role in embryonic development (Threadgill et al., 1995).

In contrast, mice engineered to individually knock out epidermal growth factor (EGF) (Luetteke et al., 1999), transforming growth factor-α (Mann et al., 1993), epigen (Dahlhoff et al., 2013), heparin binding-EGF (Jackson et al., 2003), betacellulin (BTC) (Jackson et al., 2003), or amphiregulin (Luetteke et al., 1999) reveal no lethal, ligand-specific phenotypes and all mice were viable and fertile. More subtle phenotypes include minor defects, such as altered epithelial tissue homeostasis, mammary tissue development, or a "wavy" phenotype of the hair (Ceresa et al., 2016). The distinct knockout phenotypes indicate ligand-specific roles in tissue development and homeostasis. Absence of lethality when a single ligand is knocked out is consistent with functional redundancy among the ligands for the EGFR's most critical functions. While the overlapping roles of the ligands are likely beneficial to animals, analysis of the physiological contributions of individual ligands is difficult. In order to circumvent the limitations of *in vivo* analysis we, like many others, have turned to cell biology and biochemical assays to understand ligand-specific signaling.

Among the endogenous EGFR ligands, BTC is one of the most poorly understood. It was first identified as a secreted growth factor from pancreatic β-cell insulinomas (Sasada et al., 1993; Shing et al., 1993), and has been implicated in a number of physiological processes, including β-cell proliferation (Li et al., 2001), keratinocyte proliferation (Schneider et al., 2008b), and angiogenesis (Schneider et al., 2008a). In endometrial, liver, and pancreatic cancers, BTC levels are elevated (Moon et al., 2006; Srinivasan et al., 1999; Yokoyama et al., 1995). BTC is a dual-specificity ligand that binds both EGFR and ErbB4 (Singh et al., 2016; Singh and Coffey, 2013). It has been argued that BTC also binds ErbB3 (Lopez-Torrejon et al., 2002). The most compelling evidence for this comes from 32D myeloid progenitor cells that lack endogenous ErbB RTKs. When ErbB2 and ErbB3 are exogenously expressed, there

is ErbB2 and ErbB3 tyrosine phosphorylation and increased ^{3}H-thymidine incorporation (DNA synthesis) (Alimandi et al., 1997). However, a more systematic analysis used ErbB RTKs expressed individually or in pairs; these studies demonstrated that measurable binding of BTC only occurs when EGFR and ErbB4 are expressed (Jones et al., 1999).

BTC-null mice are viable and exhibit no overt phenotypes or problems with fertility; however, the life span of these mice is reduced (Jackson et al., 2003). Overexpression of BTC causes abnormal hair follicle development (Schneider et al., 2008a), increased glucose tolerance (Dahlhoff et al., 2009), and altered corneal development (Schneider et al., 2005). In corneal epithelial cells, BTC is more efficacious than EGF in mediating wound healing (Peterson et al., 2014). Despite evidence that BTC enhances wound healing under both physiological and pathological conditions, the molecular mechanism by which BTC enhances this process is unclear. These data illustrate the long-standing, inherent confusion regarding BTC-mediated signaling, and the need for a unifying model.

In this study, we found that BTC is a better mediator of cell migration than EGF, despite a lower affinity for and reduced phosphorylation of the EGFR (Watanabe et al., 1994). The reduced receptor phosphorylation is due to the EGFR's formation of heterodimers with the kinase impaired ErbB3. Importantly, BTC promotes ErbB3 phosphorylation in the absence of ErbB2. Proximity ligation assays directly reveal the formation of EGFR:ErbB3 heterodimers. When ErbB3 signaling is antagonized or depleted using an ErbB3 antibody MM-121 (Schoeberl et al., 2009) or siRNA, cell migration is reduced more in response to BTC than EGF; further indicating BTC mediates migration through ErbB3. Together, these data provide a new model in which a ligand can bias dimerization partners of the EGFR and affect cell physiology.

Materials and Methods:

Cell lines – hTCEpi cells were obtained from Geron Corp. (Menlo Park, CA). Human corneal epithelial cells were immortalized by the stable transfection of human telomerase reverse transcriptase (Robertson et al., 2005). Cells were grown in growth media (Defined Keratinocyte with growth supplement; Invitrogen, Carlsbad, CA) at 37°C and were maintained at 5% CO_2. MDA-MB-468 cells were acquired from the ATCC. Cells were maintained in growth media [Dulbecco's Modified Eagle Medium (DMEM)] supplemented with 10% Fetal Bovine Serum (FBS), 1% penicillin, 1% streptomycin, and 2 mM glutamine all acquired from Life Technologies (Grand Island, NY). Cells were maintained at of 37 ºC in 5% CO_2.

Materials – EGF, BTC, and NRG4 were purchased from Prospec-Tany TechnoGene Ltd (Rehovot, Israel). MM-121 (seribantumab) was a kindly provided by Merrimack Pharmaceuticals, Inc, (Cambridge, MA)(Schoeberl et al., 2009). All other chemicals were purchased from Sigma-Aldrich unless otherwise noted.

Single cell growth assay - hTCEpi cells were plated at a density of 30 cells/well in a 12 well tissue culture dish in low serum media (25% growth media and 75% serum free media). Cells were grown to the eight cell stage then treated with EGF or BTC [1.6 nM] or no ligand. Photographs of the cell colonies were taken every 24 hours. At each time point, the number of cells per colony were counted and the area the colony covered was measured using Image J software (Schneider et al., 2012).

Molecular Pharmacology Fast Forward. Published on September 24, 2018 as DOI: 10.1124/mol.118.113399
This article has not been copyedited and formatted. The final version may differ from this version.

Competition binding – All radioligand binding experiments used binding buffer (DMEM (without bicarbonate), 10mM NaHEPES, 0.1% BSA, pH 7.4). Confluent 12-well dishes of hTCEpi cells were incubated with varying concentrations of cold ligand (EGF, BTC, NRG4) and ^{125}I-EGF (Perkin Elmer Life Sciences, catalog no. NEX160; specific activity 150-200 μCi/μg, ~10,000 cpm/10μl). Cells were incubated on ice for 2 hours allowing a steady state binding while preventing membrane trafficking. Cells were washed 4 times with radioligand binding buffer, solubilized in 0.1% SDS/0.1N NaOH and radioactivity level of each sample was determined using a Beckman Coulter gamma counter (Brea, CA). Data are plotted as the percentage of maximal radioactivity as determined from cells with no competitive ligand added. IC_{50} values were calculated using a one-site model using GraphPad Prism 6.05 (La Jolla, CA).

pH dissociation binding – Confluent 12-well dishes of hTCEpi cells were incubated with ^{125}I-EGF (Perkin Elmer Life Sciences, catalog no. NEX160; specific activity 150-200 μCi/μg) or ^{125}I-BTC (Perkin Elmer Life Sciences, custom synthesis; specific activity 94 μCi/μg), (~10,000 cpm/10μl). Cells were incubated on ice for 2 hours allowing a steady state distribution of the ligands. The pH of radioligand binding buffer was adjusted with NaOH or HCl to bring the buffer to the desired pH (2 – 8). pH-adjusted buffer was used to wash the cells to remove excess ligand and dissociate the ligand from the receptor. Cells were solubilized in 0.1% SDS/0.1N NaOH and the associated radioactivity in each sample was determined using a Beckman Coulter gamma counter. Data are plotted as the average (± S.D.) percentage of radioactivity relative to maximal binding.

Molecular Pharmacology Fast Forward. Published on September 24, 2018 as DOI: 10.1124/mol.118.113399
This article has not been copyedited and formatted. The final version may differ from this version.

Western blot with phospho-specific antibodies – hTCEpi cells were washed twice with PBS pH 7.4 and incubated with serum-free KSFM for 2h. Cells were treated with the indicated ligand concentration at the indicated time. Treated cells were subjected to two quick washes with PBS pH 7.4, equilibrated to 4°C on ice. Cells were harvested in lysis buffer (150 mM NaCl, 1% Nonidet P-40, 0.5% deoxycholate, 0.1% SDS, 50 mM Tris, pH 8.0, 10 mM sodium pyrophosphate, 100 mM sodium fluoride) supplemented with 2 mM Phenylmethylsulfonyl fluoride (PMSF), solubilized with end over end rotation for 10 min at 4°C. Insoluble material was removed by centrifugation for 10 min at 4°C and maximum speed (21,130 rcf) in an Eppendorf 5424R (Hamburg, Germany). Equivalent amounts of cell lysate were resolved by SDS-PAGE and transferred to nitrocellulose. The indicated proteins were immunoblotted using the following antibodies: EGFR (SC-03) and EGFR (A-10) antibodies obtained from Santa Cruz Biotechnology (Dallas, TX), site specific phosphoEGFR antibodies (pY998, pY1045, pY1068, and pY1148) were from Cell Signaling (Danvers, MA), α-tubulin antibodies were from Sigma-Aldrich (St. Louis, MO). Following incubation with the appropriate horseradish peroxidase-conjugated secondary antibody, immunoreactive proteins were visualized with Enhanced Chemiluminescence and a Fotodyne Imaging system (Hartland, WI).

Immunoprecipitations - Cell lysates (500 μg, see "Western Blot") were incubated with either a pool of phosphotyrosine antibodes (pY20, sc-508; pY99, sc-7020 from Santa Cruz Biotechnology, Santa Cruz, CA and 4G10, 05-321 from EMD Millipore, Billerica, MA**)** or ErbB3 antibodies (sc-285, sc-7390, sc-415, Santa Cruz Biotechnology, Santa Cruz, CA)[HER3/ErbB3 (D22C5) XP, Cell Signaling] while rotated end over end at 4°C overnight. Protein A/G agarose beads (Santa Cruz Biotechnology, Dallas, TX) washed with lysis buffer were added and

Molecular Pharmacology Fast Forward. Published on September 24, 2018 as DOI: 10.1124/mol.118.113399
This article has not been copyedited and formatted. The final version may differ from this version.

rotated end over end at 4°C for 2 hours. Lysates were centrifuged and a sample of the supernatant was kept as pass through (PT), the rest discarded. Then, lysis buffer was used to wash the beads three times. To elute the protein from the beads, SDS sample buffer was added to the samples and heated to 100°C for three minutes. The immunoprecipitates were divided into thirds, separated by SDS-PAGE, transferred to nitrocellulose, and detected with the indicated antibody: EGFR (Santa Cruz Biotechnology, Dallas, TX); ErbB2 and ErbB3, (Cell Signaling); ErbB3 (Santa Cruz Biotechnology, Dallas, TX, Cell Signaling), or PY99/phosphotyrosine (Santa Cruz Biotechnology, Dallas, TX) as described previously.

PLA Proximity Ligation Assay (PLA) - hTCEpi cells were plated on NaOH cleaned 12mm round #1 coverslips in a 24-well plate and grown to 70-80% confluency. Serum-starved cells were treated with media, EGF (16 nM), or BTC (16 nM) at 37°C for 15 min. Coverslips were washed with PBS^{++} (PBS pH 7.4 /0.25 M $CaCl_2$/0.25M $MgCl_2$) and fixed with 4% paraformaldehyde/PBS^{++} for 5 min on ice and 15min at room temperature. Cells were permeabilized with 0.1% saponin/0.5% fetal bovine serum/PBS^{++} for 15 min, washed 3 times in PBS^{++}. EGFR:ErbB3 heterodimers were detected using Proximity Ligation Assay kit (DuoLink, Sigma Aldrich) according to manufacturer's directions. Primary antibodies EGFR (E114, RabMAb Abcam) and ErbB3 (2F12, Thermo Scientific) were used independently and jointly as indicated in experiments. Fluorescence images and quantification were acquired using a Nikon Eclipse Ti-E widefield microscope using Nikon NIS Elements software (Nikon, Melville, NY).

Transwell migration assay - 100,000 hTCEpi cells in serum- free media (Keratinocyte Defined Media without growth supplement, 100 μL; Invitrogen) with or without 170 μg/ml MM-121.

were plated in the upper chamber of an 8 μm polycarbonate membrane, 6.5-mm insert (Corning, Inc., Corning, NY) for 2 hours at 37°C. Following incubation, the lower chamber contained 600 μL serum-free media containing the indicated concentrations of growth factor with or without MM-121 (seribantumab, a gift of Merrimack Pharmaceuticals, Cambridge, MA). Cells were allowed to migrate for 16 hours at 37°C in 5% CO2. Migrated cells were determined by fixing the cells in methanol, staining in Giemsa, and counting the migrated cells under a microscope (TE-2000; Nikon, Tokyo, Japan) with a 60X objective(Vedham et al., 2005).

siRNA – The siRNA were obtained from the following sources: scramble control siRNA (siCON), EGFR and ErbB2 were acquired from IDTDNA (Coralville, IA), ErbB3 Silencer Select was acquired from ThermoFisher Scientific, Waltham, MA) . hTCEpi cells were transfected with the indicated siRNA by Amaxa electroporation as described previously (Rush and Ceresa, 2013). Cells were allowed to recover for 48 hours. Cells were assayed by western blot for knockdown, phosphorylation of receptors or cell migration as described in materials and methods.

Statistical analyses – Statistical tests are indicated in the figure legends and were performed using GraphPad Prism 5.0 (La Jolla, CA).

Results:

BTC induces more cell migration than EGF

Our previous studies identified BTC-mediated *in vitro* corneal epithelial wound healing as significantly more robust than EGF-mediated (Peterson et al., 2014). Corneal epithelial

Molecular Pharmacology Fast Forward. Published on September 24, 2018 as DOI: 10.1124/mol.118.113399
This article has not been copyedited and formatted. The final version may differ from this version.

wound healing is a multi-faceted process that includes cell migration and proliferation (Stepp et al., 2014). The first goal for understanding the molecular basis for BTC's enhanced activity was to determine if the ligand was augmenting cell migration, cell proliferation, or both processes. To assess ligand effect on proliferation and migration, hTCEpi cells were plated as single cells and cultured in media alone or media supplemented with EGF or BTC. The same colony was photographed over 72 hours (Fig 1A). From these images, the number of cells and their total area was determined (Fig 1B, 1C). Despite no increase in cell number, BTC-treated cultures covered a larger area of the dish as compared to those grown in EGF or media alone, indicating the BTC-treated cells were more migratory.

To supplement that assay, a Transwell assay was used to directly measure cell migration in response to the growth factors (Fig 1D). BTC had a 6-fold increase in cell migration as compared to 4-fold increase with EGF. Together, these assays demonstrate that BTC stimulates cell migration more than EGF.

BTC binds EGFR with lower affinity.

BTC is universally accepted to bind both EGFR and ErbB4 (Beerli and Hynes, 1996; Riese et al., 1996), but others report that BTC can bind/activate ErbB2 and ErbB3 as well (Alimandi et al., 1997; Oh et al., 2011). hTCEpi cells do not express ErbB4 (Peterson et al., 2014), so we restricted our focus to the EGFR. To determine if EGF and BTC were binding the same receptor, we performed an ^{125}I-EGF competition binding assay. EGF, BTC, and Neuregulin 4 (NRG4) as a negative control, were used to compete for radiolabeled EGF (Fig 2A). EGF (IC_{50}= ~2 nM) was able to compete for ^{125}I-EGF binding with a 30-fold higher affinity than BTC (IC_{50}= ~60 nM); 100 nM NRG4 was unable to displace ^{125}I-EGF binding, consistent with its

Molecular Pharmacology Fast Forward. Published on September 24, 2018 as DOI: 10.1124/mol.118.113399
This article has not been copyedited and formatted. The final version may differ from this version.

role as an ErbB4 specific ligand (Fig 2A). These data indicate that EGF and BTC compete for the same binding site and BTC has a lower affinity for the EGFR.

Next, we examined whether EGFR binding of BTC and EGF, had differing sensitivities to pH. As the ligand:receptor complex progresses through the endocytic pathway, it moves through an increasingly acidic environment. Ligand binding is one of the factors that determines whether the receptor recycles back to the plasma membrane or is targeted to the lysosome. Approximately 50% of bound ^{125}I-EGF dissociated at pH 5.8, whereas a pH of 4.3 was required to dissociate 50% of the bound ^{125}I-BTC (Fig 2B). These values led to the prediction that ~50% of EGF:EGFR complexes will dissociate in the early endosome [pH ~5.9-6.8 (Yamashiro and Maxfield, 1987)], whereas, the BTC:EGFR is not predicted to have appreciable dissociation, even in the lysosome [pH ~ 4.5-5.0 (Yamashiro and Maxfield, 1987)].

BTC induces less EGFR phosphorylation but more ErbB3 phosphorylation

Consistent with the reduced affinity, BTC was a weaker activator of EGFR, as compared to EGF. Using ligand concentrations that produced maximal cell migration (Peterson et al., 2014), a time course of tyrosine phosphorylation was used as a read-out of EGFR activity (Fig 3). hTCEpi cells treated with BTC as compared to those treated with EGF had reduced EGFR phosphorylation at all four of the tyrosine residues examined (Fig 3A). Similar trends were observed in MDA-MB-468 cells, a metastatic breast cancer cell-line with comparable levels of EGFR (Fig 3B). It should be noted that supraphysiological concentrations of BTC and EGF produce comparable levels of EGFR phosphorylation (Peterson et al., 2014). The differences in EGFR phosphorylation were revealed using ligand concentrations (1.6 nM)

that produce the greatest biological response (Peterson et al., 2014), more closely reflect physiological concentrations (Peterson et al., 2014), and are closer to the ligands' K_d's for the EGFR (Schlessinger, 1986; Watanabe et al., 1994).

The decrease in EGFR phosphorylation led us to an alternative explanation. We hypothesized that EGF promoted EGFR homodimers, whereas BTC preferentially formed EGFR:ErbB3 heterodimers. The model accounts for the observation that 1) the ligands can compete for binding with one another (Jones et al., 1999; Macdonald-Obermann and Pike, 2014), 2) the EGFR:ErbB3 heterodimers would have reduced EGFR phosphorylation due to ErbB3 being kinase impaired (Guy et al., 1994), and 3) ErbB3 activation is associated with induced proliferation and migration (Lyons et al., 2005; Reschke et al., 2008; Sathyamurthy et al., 2015).

To test whether BTC could differentially signal through other ErbB receptors, we examined receptor tyrosine phosphorylation (Fig 4A-C). hTCEpi cells were treated with media alone, or media supplemented with EGF or BTC. For these biochemical experiments, higher concentrations of ligand were used to drive receptor dimerization and enhance the signal to noise ratio. Denatured cell lysates were immunoprecipitated with an anti-phosphotyrosine antibody and probed for the presence of the three endogenous ErbB receptors (Fig 4A). BTC treatment led to decreased phosphorylation of EGFR and ErbB2 when compared to EGF, whereas only BTC treatment resulted in significant ErbB3 phosphorylation (Fig 4D). Significant ErbB3 phosphorylation by BTC was also observed when cell lysates were immunoprecipitated using an ErbB3 antibody and immunoblotted with an anti-phosphotyrosine antibody (Fig 4B, 4E).

hTCEpi cells were transduced using ErbB2-specific shRNA to examine the possibility of ErbB2 involvement in ErbB3 phosphorylation. BTC-mediated activation of ErbB3 is unaffected by the loss of ErbB2 (calculated to be 86% knockdown), further indicating that ErbB2 is dispensable in BTC activation of ErbB3 (Fig 4C, 4F). To determine whether these observations were specific to hTCEpi cells, we treated MDA-MB-468 cells with EGF and BTC, and then immunoprecipitated phosphorylated tyrosines and immunoblotted for the same three ErbB receptors available in hTCEpi cells (Supplemental Fig 1A-D). MDA-MB-468 cells express EGFR and ErbB3, but do not express detectable levels of ErbB2 or ErbB4 (Khan et al., 2010). As with the hTCEpi cells, BTC treatment resulted in less EGFR tyrosine phosphorylation, and induced ErbB3 tyrosine phosphorylation.

BTC promotes ErbB3 phosphorylation and EGFR:ErbB heterodimers

These biochemical data provide evidence that BTC causes ErbB3 phosphorylation, but do not demonstrate a direct interaction. Another possibility is ErbB3 phosphorylation is mediated by a non-receptor kinase that is activated by the liganded EGFR. To determine if BTC caused an increase in EGFR:ErbB3 heterodimers, we performed proximity ligation assays (PLA) (Fig 5). PLA is an antibody based detection/amplification system that will reveal protein:protein interactions when they are within 40 nm. hTCEpi cells were treated with media alone, or media supplemented with EGF or BTC, fixed and subjected to the PLA protocol (see Experimental Procedures). When cells were screened for the presence of EGFR:ErbB3 heterodimers, EGF produced a 1.1 fold increase in heterodimers, and BTC produced a 2.6-fold increase. Together, the receptor phosphorylation data and the PLA

Molecular Pharmacology Fast Forward. Published on September 24, 2018 as DOI: 10.1124/mol.118.113399
This article has not been copyedited and formatted. The final version may differ from this version.

support the notion that EGF treated cells have less EGFR:ErbB3 heterodimer interactions when compared to those treated with BTC.

Inhibition of ErbB3 preferentially attenuates BTC-mediated cell migration

Finally, we wanted to determine if the EGFR:ErbB3 heterodimers were responsible for the increase in cell mobility that was seen with BTC treatment. We monitored ligand-dependent cell migration using a Transwell migration assay in the absence and presence of the ErbB3 antagonist antibody, MM-121 (seribantumab)(Schoeberl et al., 2009)(Fig 6). In the presence MM-121, BTC treated cells no longer migrated more than EGF treated cells.

To determine the contribution of ErbB family members on BTC-mediated migration, we knocked down EGFR, ErbB2, and ErbB3 (Fig. 6B) individually. Transfection of hTCEpi cells with these siRNA attenuated expression of EGFR, ErbB2 and ErbB3 by 49%, 78% and 91% respectively. The decreased levels of ErbB3 eliminated the significant BTC mediated migration advantage when compared to EGF (Fig. 6C). The loss of any of the three ErbB RTKs decreases the advantage of BTC treatment over EGF (Fig. 6C). These data are consistent with all ErbB family members contributing to BTC-mediated signaling.

Discussion:

In this manuscript, we demonstrate that EGFR-related growth factors differ in their ability to induce phosphorylation, direct specific receptor dimerization and effect cell physiology. Multiple labs have reported that BTC treatment can generate a greater response than EGF (Beerli and Hynes, 1996; Knudsen et al., 2014; Peterson et al., 2014; Schoeberl et al., 2009). We show that in line with those findings, BTC enhances cell migration more than EGF (Fig 1

and 6), which is a fundamental component of corneal wound healing (Fig 1 and 6). Furthermore, this effect is not due to enhanced BTC binding to or phosphorylation of the EGFR (Fig 2 - 4), as these responses are reduced with BTC treatment.

Rather, BTC binding to the EGFR biases the receptor to heterodimerize with ErbB3, resulting in ErbB3 phosphorylation (Fig 3-5,1S). Importantly, BTC-mediated ErbB3 phosphorylation is independent of ErbB2. These heterodimers contribute to cell migration, as ErbB3 antagonists and knockdown inhibit BTC-mediated migration to a greater extent than EGF-mediated migration (Fig 6).

We propose a model in which EGF and BTC both bind the EGFR, but differentially bias the dimerization partner of the ligand-bound receptor. This ligand-biased signaling is well established among G-protein coupled receptors (Kinzer-Ursem and Linderman, 2007; Luttrell and Kenakin, 2011; Zidar et al., 2009). In the cell, monomeric ErbB RTKs and their ligands are in a biochemical equilibrium. The binding of ligand shifts the equilibrium of the receptors from a monomeric to a dimeric form. Our data here support a model in which the ligand:EGFR directs whether the dimers are homodimers or heterodimers. There is an additional layer of complexity to this model when applying it to other cell lines, which express the ErbB RTKs at different levels.

Reports in the literature have been inconsistent regarding how BTC induces ErbB3 phosphorylation (Chiba, 2004; Pinkas-Kramarski et al., 1996; Riese et al., 1996; Riese et al., 1995; Steinkamp et al., 2014). We postulate that the absolute and relative amounts of EGFR and ErbB3 in different cell lines are a potential source for these discrepancies. Since BTC drives the formation of EGFR:ErbB3 heterodimers, if EGFRs are in vast excess, once the maximum number of heterodimers are formed, the remaining liganded EGFRs are able to

form homodimers or ErbB2 heterodimers. These dimers may mask the contribution of EGFR:ErbB3 heterodimer. Our data support this hypothesis, as the loss of EGFR and ErbB2 also decreased the significant advantage BTC treatment had on migration (Fig 6). hTCEpi cells have sufficient levels of EGFR and ErbB3 to produce functional EGFR:ErbB3 heterodimers, as evident by the decreased cell migration in response to ErbB3 antagonist and ErbB3 knockdown. Cells that do not express ErbB3 may not show differences in responses to EGF and BTC.

Several previous studies support this model. First, Liu et al. report that a single ligand is sufficient to activate EGFR dimers (Liu et al., 2012). While this is well accepted for ErbB RTKs that heterodimerize with the ligandless ErbB2, it is important to note that it can extend to the other family members that undergo conformational changes to dimerize. Second, our findings that receptors preferentially form dimer partners is supported by the work of MacDonald-Oberman et al. (Macdonald-Obermann et al., 2013; Macdonald-Obermann and Pike, 2014). Our endogenous receptor model proposes that these preferences can be shifted by the activating ligand. As indicated from our PLA experiments, BTC preferentially drives the formation of EGFR:ErbB3.

It was fortunate that hTCEpi and MDA-MB-468 cells do not express ErbB4, another target for BTC binding. With the addition of ErbB4, the model would have to take into consideration the binding affinities for EGFR versus ErbB4. Although ErbB2 does not bind BTC, its contribution cannot be overlooked. It is likely that ErbB2 is also competing for binding to the liganded EGFRs. ErbB3 phosphorylation was unaffected by the loss of ErbB2, further supporting EGFR as the sole ligand binding receptor in our system. The incomplete inhibition of ErbB3 initiated migration in response to MM-121 may be due to compensatory

Molecular Pharmacology Fast Forward. Published on September 24, 2018 as DOI: 10.1124/mol.118.113399
This article has not been copyedited and formatted. The final version may differ from this version.

ErbB2 effects. The knockdown of each ErbB RTK had an increase in protein levels of the other ErbB RTKs when compared to control lysates, especially with EGFR knockdown (Fig. 6B). Other groups show that compensatory protein effects following knockdown of similar proteins are possible and support this phenomenon (Krumins and Gilman, 2006; Rossi et al., 2015). This effect was also supported in the receptor knockout cell lines where the loss of EGFR, ErbB2 and ErbB3 decreased the migration advantage BTC has over EGF. While ErbB2 is not necessary to activate ErbB3 with BTC, it contributes to BTC-mediated migration, similar to ErbB3 (Fig 6C). More rigorous mathematical modeling and experimentation are required to account for the complexities of the entire ErbB RTK family.

While it has been previously appreciated that ligands can direct dimer formation, it was largely attributed to differences between which receptor the ligand bound (Macdonald-Obermann and Pike, 2014); our model proposes that two different ligands are binding the same receptor, but forming different heterodimer populations. How would ligand binding direct the dimerization partner? One possibility is that human EGF and BTC have limited sequence similarity (~36%) as well as low predicted three-dimensional structural homology as measured by solvent accessibility surfaces (Lopez-Torrejon et al., 2002). Alternatively, the size of the ligand may affect receptor conformation. The processed form of BTC is 9 kDa and EGF is 6.6 kDa (Harris et al., 2003). A stretch of ~50 amino acids directly binds to the ligand-binding domain of the receptor (Seno et al., 1996). The size and/or charge of the remaining 30 amino acids may sterically hinder BTC:EGFR homodimerization. Fundamental differences in binding are supported by our observed differences in radioligand competition binding and pH sensitivity for the two ligands (Fig 2).

Conclusion:

The physiological significance of individual ErbB RTK ligands is likely important as indicated by knockout animals. Using cell culture models, we were able to dissect how EGF and BTC can form different ErbB receptor combinations and elicit specific cell biological responses. We propose a new model for how BTC binding to the EGFR biases it in the formation of EGFR:ErbB3 heterodimers. These heterodimers are distinct from EGFR homodimers in their ability to enhance cell migration despite less EGFR phosphorylation. This model may have important implications in the prognosis of cancer. Many cancers are characterized by the overexpression of individual ErbB family members and specific ErbB ligands (Hynes and MacDonald, 2009). Based on the evidence that ligand binding affects receptor dimerization and the resulting cell biology, assessing receptor levels and local levels of growth factor may predict the invasiveness of the cancer.

Authorship Contributions:

Participated in research design: Rush, Peterson, Ceresa

Conducted experiments: Rush, Peterson

Contributed new reagents or analytical tools: Rush, Peterson

Performed data analysis: Rush, Peterson, Ceresa

Wrote or contributed to the writing of the manuscript: Rush, Peterson, Ceresa

Molecular Pharmacology Fast Forward. Published on September 24, 2018 as DOI: 10.1124/mol.118.113399
This article has not been copyedited and formatted. The final version may differ from this version.

References

Alimandi M, Wang LM, Bottaro D, Lee CC, Kuo A, Frankel M, Fedi P, Tang C, Lippman M and Pierce JH (1997) Epidermal growth factor and betacellulin mediate signal transduction through co-expressed ErbB2 and ErbB3 receptors. *The EMBO journal* **16**(18): 5608-5617.

Beerli RR and Hynes NE (1996) Epidermal growth factor-related peptides activate distinct subsets of ErbB receptors and differ in their biological activities. *The Journal of biological chemistry* **271**(11): 6071-6076.

Ceresa BP, Gosney JA, Jackson NM and Rush JS (2016) Epidermal Growth Factor Receptor, in *Encyclopedia of Signaling Molecules* pp 1-11, Springer New York : New York, NY.

Chen JC, Zeng FH, Forrester SJ, Eguchi S, Zhang MZ and Harris RC (2016) Expression and Function of the Epidermal Growth Factor Receptor in Physiology and Disease. *Physiol Rev* **6**(3): 1025-1069.

Chiba T (2004) What are the real roles of different erbB proteins in Barrett's Esophagus. *Digestion* **70**(2): 93-94.

Dahlhoff M, Dames PM, Lechner A, Herbach N, van Burck L, Wanke R, Wolf E and Schneider MR (2009) Betacellulin overexpression in transgenic mice improves glucose tolerance and enhances insulin secretion by isolated islets in vitro. *Molecular and cellular endocrinology* **299**(2): 188-193.

Dahlhoff M, Schafer M, Wolf E and Schneider MR (2013) Genetic deletion of the EGFR ligand epigen does not affect mouse embryonic development and tissue homeostasis. *Experimental cell research* **319**(4): 529-535.

Guy PM, Platko JV, Cantley LC, Cerione RA and Carraway KL, 3rd (1994) Insect cell-expressed p180erbB3 possesses an impaired tyrosine kinase activity. *Proceedings of the National Academy of Sciences of the United States of America* **91**(17): 8132-8136.

Harris RC, Chung E and Coffey RJ (2003) EGF Receptor ligands. *Experimental cell research* **284**(1): 2-13.

Hynes NE and MacDonald G (2009) ErbB receptors and signaling pathways in cancer. *Current opinion in cell biology* **21**(2): 177-184.

Jackson LF, Qiu TH, Sunnarborg SW, Chang A, Zhang C, Patterson C and Lee DC (2003) Defective valvulogenesis in HB-EGF and TACE-null mice is associated with aberrant BMP signaling. *The EMBO journal* **22**(11): 2704-2716.

Jones JT, Akita RW and Sliwkowski MX (1999) Binding specificities and affinities of egf domains for ErbB receptors. *FEBS letters* **447**(2-3): 227-231.

Khan IH, Zhao J, Ghosh P, Ziman M, Sweeney C, Kung HJ and Luciw PA (2010) Microbead arrays for the analysis of ErbB receptor tyrosine kinase activation and dimerization in breast cancer cells. *Assay and drug development technologies* **8**(1): 27-36.

Kinzer-Ursem TL and Linderman JJ (2007) Both ligand- and cell-specific parameters control ligand agonism in a kinetic model of g protein-coupled receptor signaling. *PLoS computational biology* **3**(1): e6.

Knudsen SL, Mac AS, Henriksen L, van Deurs B and Grovdal LM (2014) EGFR signaling patterns are regulated by its different ligands. *Growth Factors* **32**(5): 155-163.

Krumins AM and Gilman AG (2006) Targeted knockdown of G protein subunits selectively prevents receptor-mediated modulation of effectors and reveals complex changes in

non-targeted signaling proteins. *The Journal of biological chemistry* **281**(15): 10250-10262.

Li L, Seno M, Yamada H and Kojima I (2001) Promotion of beta-cell regeneration by betacellulin in ninety percent-pancreatectomized rats. *Endocrinology* **142**(12): 5379-5385.

Liu P, Cleveland TEt, Bouyain S, Byrne PO, Longo PA and Leahy DJ (2012) A single ligand is sufficient to activate EGFR dimers. *Proceedings of the National Academy of Sciences of the United States of America* **109**(27): 10861-10866.

Lopez-Torrejon I, Querol E, Aviles FX, Seno M, de Llorens R and Oliva B (2002) Human betacellulin structure modeled from other members of EGF family. *J Mol Model* **8**(4): 131-144.

Luetteke NC, Qiu TH, Fenton SE, Troyer KL, Riedel RF, Chang A and Lee DC (1999) Targeted inactivation of the EGF and amphiregulin genes reveals distinct roles for EGF receptor ligands in mouse mammary gland development. *Development (Cambridge, England)* **126**(12): 2739-2750.

Luttrell LM and Kenakin TP (2011) Refining Efficacy: Allosterism and Bias in G Protein-Coupled Receptor Signaling, in *Signal Transduction Protocols* (Luttrell LM and Ferguson SSG eds) pp 3-35, Humana Press, Totowa, NJ.

Lyons DA, Pogoda HM, Voas MG, Woods IG, Diamond B, Nix R, Arana N, Jacobs J and Talbot WS (2005) erbb3 and erbb2 are essential for schwann cell migration and myelination in zebrafish. *Current biology : CB* **15**(6): 513-524.

Macdonald-Obermann JL, Adak S, Landgraf R, Piwnica-Worms D and Pike LJ (2013) Dynamic analysis of the epidermal growth factor (EGF) receptor-ErbB2-ErbB3 protein network by luciferase fragment complementation imaging. *The Journal of biological chemistry* **288**(42): 30773-30784.

Macdonald-Obermann JL and Pike LJ (2014) Different epidermal growth factor (EGF) receptor ligands show distinct kinetics and biased or partial agonism for homodimer and heterodimer formation. *The Journal of biological chemistry* **289**(38): 26178-26188.

Mann GB, Fowler KJ, Gabriel A, Nice EC, Williams RL and Dunn AR (1993) Mice with a null mutation of the TGF alpha gene have abnormal skin architecture, wavy hair, and curly whiskers and often develop corneal inflammation. *Cell* **73**(2): 249-261.

Moon WS, Park HS, Yu KH, Park MY, Kim KR, Jang KY, Kim JS and Cho BH (2006) Expression of betacellulin and epidermal growth factor receptor in hepatocellular carcinoma: implications for angiogenesis. *Human pathology* **37**(10): 1324-1332.

Oh YS, Shin S, Lee Y-J, Kim EH and Jun H-S (2011) Betacellulin-Induced Beta Cell Proliferation and Regeneration Is Mediated by Activation of ErbB-1 and ErbB-2 Receptors. *PLOS ONE* **6**(8): e23894.

Pathak BG, Gilbert DJ, Harrison CA, Luetteke NC, Chen X, Klagsbrun M, Plowman GD, Copeland NG, Jenkins NA and Lee DC (1995) Mouse chromosomal location of three EGF receptor ligands: amphiregulin (Areg), betacellulin (Btc), and heparin-binding EGF (Hegfl). *Genomics* **28**(1): 116-118.

Peterson JL, Phelps ED, Doll MA, Schaal S and Ceresa BP (2014) The role of endogenous epidermal growth factor receptor ligands in mediating corneal epithelial homeostasis. *Investigative ophthalmology & visual science* **55**(5): 2870-2880.

Pinkas-Kramarski R, Soussan L, Waterman H, Levkowitz G, Alroy I, Klapper L, Lavi S, Seger R, Ratzkin BJ, Sela M and Yarden Y (1996) Diversification of Neu differentiation factor and epidermal growth factor signaling by combinatorial receptor interactions. *The EMBO journal* **15**(10): 2452-2467.

Reschke M, Mihic-Probst D, van der Horst EH, Knyazev P, Wild PJ, Hutterer M, Meyer S, Dummer R, Moch H and Ullrich A (2008) HER3 Is a Determinant for Poor Prognosis in Melanoma. *Clinical Cancer Research* **14**(16): 5188-5197.

Riese DJ, 2nd, Bermingham Y, van Raaij TM, Buckley S, Plowman GD and Stern DF (1996) Betacellulin activates the epidermal growth factor receptor and erbB-4, and induces cellular response patterns distinct from those stimulated by epidermal growth factor or neuregulin-beta. *Oncogene* **12**(2): 345-353.

Riese DJ, 2nd, van Raaij TM, Plowman GD, Andrews GC and Stern DF (1995) The cellular response to neuregulins is governed by complex interactions of the erbB receptor family. *Molecular and cellular biology* **15**(10): 5770-5776.

Robertson DM, Li L, Fisher S, Pearce VP, Shay JW, Wright WE, Cavanagh HD and Jester JV (2005) Characterization of Growth and Differentiation in a Telomerase-Immortalized Human Corneal Epithelial Cell Line. *Inv Opth Vis Sci* **46**(2): 470-478.

Rossi A, Kontarakis Z, Gerri C, Nolte H, Hölper S, Krüger M and Stainier DYR (2015) Genetic compensation induced by deleterious mutations but not gene knockdowns. *Nature* **524**: 230.

Rush JS and Ceresa BP (2013) RAB7 and TSG101 are required for the constitutive recycling of unliganded EGFRs via distinct mechanisms. *Molecular and cellular endocrinology* **381**(1-2): 188-197.

Sasada R, Ono Y, Taniyama Y, Shing Y, Folkman J and Igarashi K (1993) Cloning and expression of cDNA encoding human betacellulin, a new member of the EGF family. *Biochemical and biophysical research communications* **190**(3): 1173-1179.

Sathyamurthy A, Yin DM, Barik A, Shen C, Bean JC, Figueiredo D, She JX, Xiong WC and Mei L (2015) ERBB3-mediated regulation of Bergmann glia proliferation in cerebellar lamination. *Development (Cambridge, England)* **142**(3): 522-532.

Schlessinger J (1986) Allosteric regulation of the epidermal growth factor receptor kinase. *The Journal of cell biology* **103**(6 Pt 1): 2067-2072.

Schneider CA, Rasband WS and Eliceiri KW (2012) NIH Image to ImageJ: 25 years of image analysis. *Nat Methods* **9**(7): 671-675.

Schneider MR, Antsiferova M, Feldmeyer L, Dahlhoff M, Bugnon P, Hasse S, Paus R, Wolf E and Werner S (2008a) Betacellulin regulates hair follicle development and hair cycle induction and enhances angiogenesis in wounded skin. *J Invest Dermatol* **128**(5): 1256-1265.

Schneider MR, Dahlhoff M, Herbach N, Renner-Mueller I, Dalke C, Puk O, Graw J, Wanke R and Wolf E (2005) Betacellulin overexpression in transgenic mice causes disproportionate growth, pulmonary hemorrhage syndrome, and complex eye pathology. *Endocrinology* **146**(12): 5237-5246.

Schneider MR, Werner S, Paus R and Wolf E (2008b) Beyond wavy hairs: the epidermal growth factor receptor and its ligands in skin biology and pathology. *The American journal of pathology* **173**(1): 14-24.

Schoeberl B, Pace EA, Fitzgerald JB, Harms BD, Xu L, Nie L, Linggi B, Kalra A, Paragas V, Bukhalid R, Grantcharova V, Kohli N, West KA, Leszczyniecka M, Feldhaus MJ, Kudla AJ and Nielsen UB (2009) Therapeutically targeting ErbB3: a key node in ligand-induced activation of the ErbB receptor-PI3K axis. *Science signaling* **2**(77): ra31.

Seno M, Tada H, Kosaka M, Sasada R, Igarashi K, Shing Y, Folkman J, Ueda M and Yamada H (1996) Human betacellulin, a member of the EGF family dominantly expressed in pancreas and small intestine, is fully active in a monomeric form. *Growth Factors* **13**(3-4): 181-191.

Shing Y, Christofori G, Hanahan D, Ono Y, Sasada R, Igarashi K and Folkman J (1993) Betacellulin: a mitogen from pancreatic beta cell tumors. *Science (New York, NY)* **259**(5101): 1604-1607.

Singh B, Carpenter G and Coffey RJ (2016) EGF receptor ligands: recent advances. *F1000Res* **5**.

Singh B and Coffey RJ (2013) Trafficking of Epidermal Growth Factor Receptor Ligands in Polarized Epithelial Cells. *Annu Rev Physiol*.

Srinivasan R, Benton E, McCormick F, Thomas H and Gullick WJ (1999) Expression of the c-erbB-3/HER-3 and c-erbB-4/HER-4 growth factor receptors and their ligands, neuregulin-1 alpha, neuregulin-1 beta, and betacellulin, in normal endometrium and endometrial cancer. *Clin Cancer Res* **5**(10): 2877-2883.

Steinkamp MP, Low-Nam ST, Yang S, Lidke KA, Lidke DS and Wilson BS (2014) erbB3 is an active tyrosine kinase capable of homo- and heterointeractions. *Molecular and cellular biology* **34**(6): 965-977.

Stepp MA, Zieske JD, Trinkaus-Randall V, Kyne BM, Pal-Ghosh S, Tadvalkar G and Pajoohesh-Ganji A (2014) Wounding the cornea to learn how it heals. *Experimental eye research* **121**: 178-193.

Threadgill DW, Dlugosz AA, Hansen LA, Tennenbaum T, Lichti U, Yee D, LaMantia C, Mourton T, Herrup K, Harris RC and et al. (1995) Targeted disruption of mouse EGF receptor: effect of genetic background on mutant phenotype. *Science (New York, NY)* **269**(5221): 230-234.

Vedham V, Phee H and Coggeshall KM (2005) Vav Activation and Function as a Rac Guanine Nucleotide Exchange Factor in Macrophage Colony-Stimulating Factor-Induced Macrophage Chemotaxis. *Molecular and cellular biology* **25**(10): 4211-4220.

Wang YN and Hung MC (2012) Nuclear functions and subcellular trafficking mechanisms of the epidermal growth factor receptor family. *Cell Biosci* **2**(1): 13.

Watanabe T, Shintani A, Nakata M, Shing Y, Folkman J, Igarashi K and Sasada R (1994) Recombinant human betacellulin. Molecular structure, biological activities, and receptor interaction. *The Journal of biological chemistry* **269**(13): 9966-9973.

Wieduwilt MJ and Moasser MM (2008) The epidermal growth factor receptor family: biology driving targeted therapeutics. *Cell Mol Life Sci* **65**(10): 1566-1584.

Wiley HS (2003) Trafficking of the ErbB Receptors and its Influence on Signaling. *Experimental cell research* **284**(1): 78-88.

Yamashiro DJ and Maxfield FR (1987) Acidification of morphologically distinct endosomes in mutant and wild-type Chinese hamster ovary cells. *The Journal of cell biology* **105**(6 Pt 1): 2723-2733.

Yokoyama M, Funatomi H, Kobrin M, Ebert M, Friess H, Buchler M and Korc M (1995) Betacellulin, a member of the epidermal growth-factor family, is overexpressed in human pancreatic-cancer. *Int J Oncol* **7**(4): 825-829.

Zidar DA, Violin JD, Whalen EJ and Lefkowitz RJ (2009) Selective engagement of G protein coupled receptor kinases (GRKs) encodes distinct functions of biased ligands. *Proceedings of the National Academy of Sciences* **106**(24): 9649-9654.

Footnotes. JLP's current affiliation is Arkansas College of Osteopathic Medicine. This work was supported by National Institutes of Health Grants [1R01EY021497] (BPC) and [R21EY027032] (BPC).

Molecular Pharmacology Fast Forward. Published on September 24, 2018 as DOI: 10.1124/mol.118.113399
This article has not been copyedited and formatted. The final version may differ from this version.

Figure Legends.

Figure 1. BTC is a more efficacious activator of cell migration than EGF. A-C) hTCEpi cells were plated as single cells (30 cells/35 mm dish) in media alone, 1.6 nM EGF, or 1.6 nM BTC. A) Once cell colonies formed, they were imaged at 24 hour intervals for 72 hours. Shown are representative data from an experiment repeated three times (~25-70 colonies for each condition). Scale bar = 200 μm. B) Data from three separate experiments were plotted as average ± S.D. fold change as number of cells per colony. C) Data from three separate experiments were plotted as average ± S.D. fold change in area per cell. D) hTCEpi cell migration was measured using a Transwell assay after migrating for 16 hours as described in Experimental Procedures. Cells were incubated in serum free media with no additions (Media), serum (Serum), 1.6 nM EGF, or 1.6 nM BTC. Plotted are the fold changes (average ± S.D.) in cell migration (relative to serum free media) for each condition (n=6). Data were analyzed using a two-way ANOVA with a Tukey's post-hoc analysis. *= $p<0.05$ and ** = $p<0.01$.

Figure 2. BTC and EGF bind EGFRs with different affinities and pH sensitivities. A) ^{125}I-EGF competition binding using varying concentrations of EGF, BTC, or NRG4 as indicated. B) pH sensitivity of ^{125}I-EGF and ^{125}I-BTC binding. Cells were incubated with radioligand at pH 7.4 and 4°C until steady-state binding was achieved. Cells were then incubated in binding buffer at varying pH at 4°C for 30 minutes, then washed three times in ice cold buffer of the same pH. Cells were solubilized and associated radioactivity was measured. For (A-B), data are plotted as the percent of maximal radioligand binding (average ± S.D., n=3).

Figure 3. BTC induces less EGFR phosphorylation than EGF in hTCEpi and MDA-MB-468 cells. A-B) Cells were treated with 1.6 nM EGF or 1.6 nM BTC for the indicated times. Cell lysates were prepared and immunobloted with the indicated EGFR phosphotyrosine specific antibodies (pY998, pY1045, pY1068, pY1148), total EGFR, or α-tubulin. A) hTCEpi cell representative blots from three experiments. B) MDA-MB-468 cell representative blots from three experiments.

Figure 4. BTC induces ErbB3 phosphorylation in hTCEpi cells without ErbB2 interaction. A-C) hTCEpi were treated with serum free media alone, 16 nM EGF, or 16 nM BTC for 15 min as indicated. Cell lysates were prepared under denaturing conditions and the indicated proteins were immunoprecipitated using A) anti-phosphotyrosine or B) anti-ErbB3 antibodies. The pass-through (PT) and immunoprecipitates were resolved by 7.5% SDS-PAGE, and immunoblotted with the indicated antibodies. Shown are representative blots from an experiment performed at least three times. C) Transduced ErbB2-shRNA and shRNA control (materials and methods) hTCEpi cells were treated the same as A-B. Shown are representative blots from three replicates. D-F) Immunoblots from A-C were quantified using NIH Image J. Data are presented as the average ratio (± S.D.) of each treatment to the most abundant protein. Blots were analyzed with a two-way ANOVA, Holm-Sidak's multiple comparisons test. * = $p < 0.05$, ** = $p < 0.01$, *** = $p < 0.001$ NS= not significant.

Molecular Pharmacology Fast Forward. Published on September 24, 2018 as DOI: 10.1124/mol.118.113399
This article has not been copyedited and formatted. The final version may differ from this version.

Figure 5. **BTC induces EGFR:ErbB3 heterodimers in hTCEpi cells.** EGFR:EGFR or EGFR:ErbB3 dimerization was visualized by proximity ligation assay (PLA). After serum starving cells for 2 hrs, hTCEpi cells were treated with serum free media alone or with 16nM EGF or BTC for 15min at 37°C. After treatment, cells were fixed and probed using the proximity ligation assay (PLA) as described in Material and Methods. A) Representative micrographs of cells probed for EGFR:ErbB3 heterodimers. B) Data from three independent experiments were quantified (50-100 cells/experiment) and are presented as a box and whisker plot of the total number of signals per cell and analyzed with a one-way ANOVA, Holm-Sidak's multiple comparisons test. * = $p < 0.05$.

Figure 6. **ErbB3 antagonist MM-121 and knockdown inhibit BTC-mediated migration to a greater extent than EGF-mediated migration.** A) hTCEpi cells were plated on the upper chamber of transwells (0.8 nm pore) and pre-treated without or with 170 μg/ml MM-121 for 2 hours. The media was replaced with 1) serum free media alone, 2) EGF (1.6 nM) or 3) BTC (1.6 nM) in the absence or presence of MM-121. Cells were incubated for 16 hours and migration to the lower chamber was measured by counting the number of migrated cells on the underside of the membrane. Shown are the results of 6 independent experiments for each condition. B) hTCEpi cells were transfected with either control siRNA (siCON) or siRNA specific for EGFR, ErbB2 or ErB3 as described in Materials and Methods. After recovery (72h), B) immunoblots from cell lysates were prepared from hTCEpi samples, and equal amounts of total protein loaded. Samples were resolved by SDS-PAGE and immunoblotted with the indicated antibody. Immunoblots shown are representative from experiments performed at least 6 times. C) transwells were loaded with transfected cells as described in

Materials and Methods. Migrated cells were quantified and each experiment normalized to media treated cells independently. Each y-axis indicates a different transfected hTCEpi cell-line. The results are plotted as mean ± S.D. Data were analyzed with a two-way ANOVA with Holm-Sidak's post-hoc analysis, * = $p < 0.05$, NS= not significant.

Figure 1

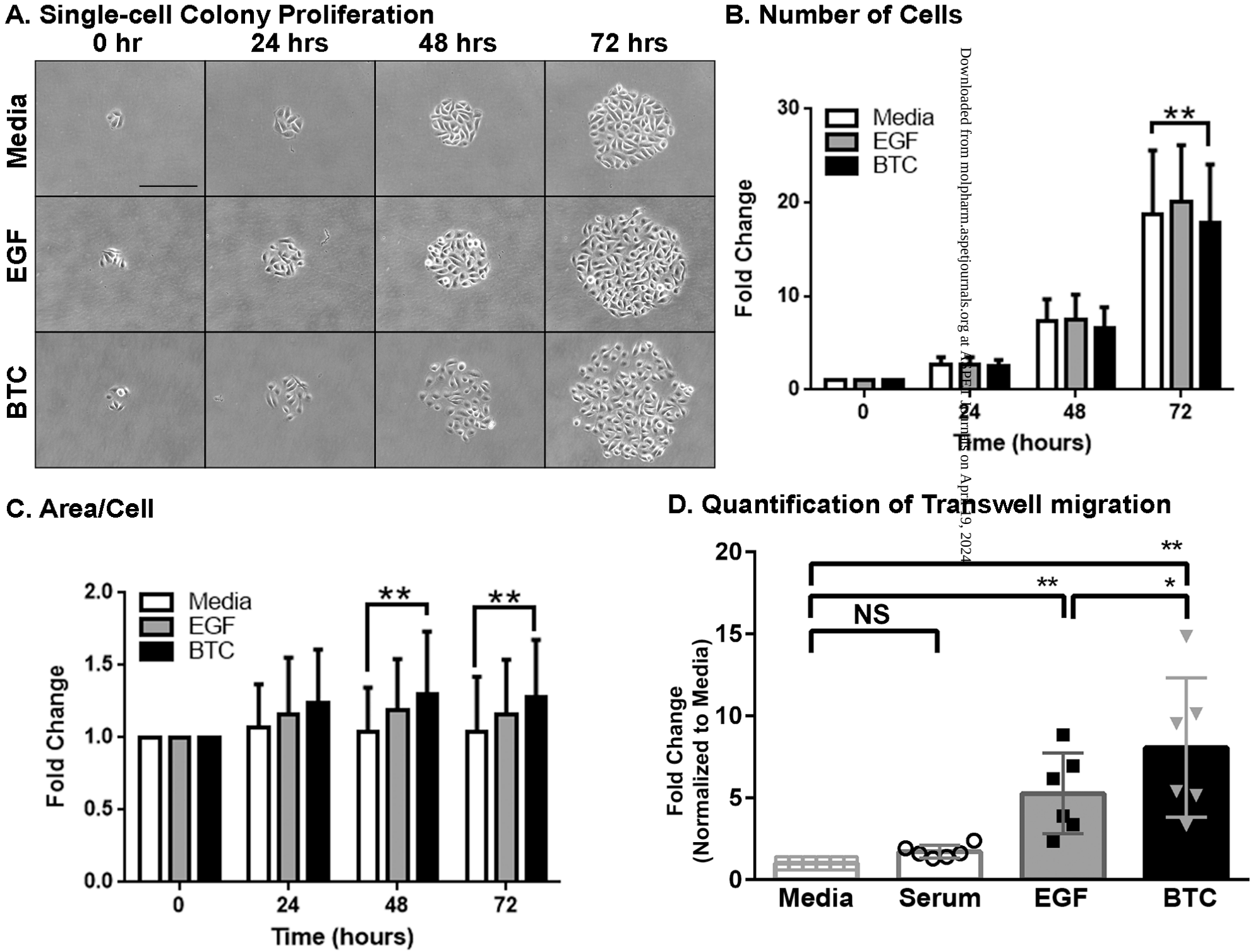

Figure 2

A. ^{125}I-EGF Competition binding

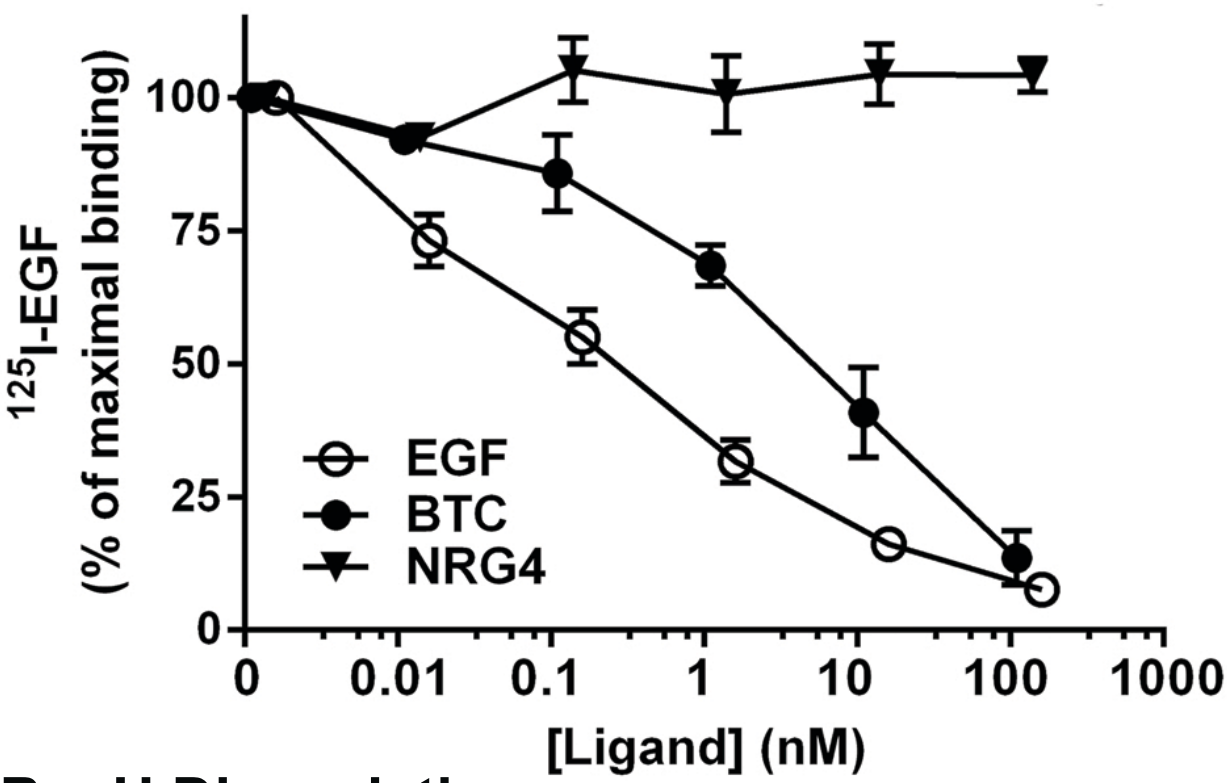

B. pH Dissociation

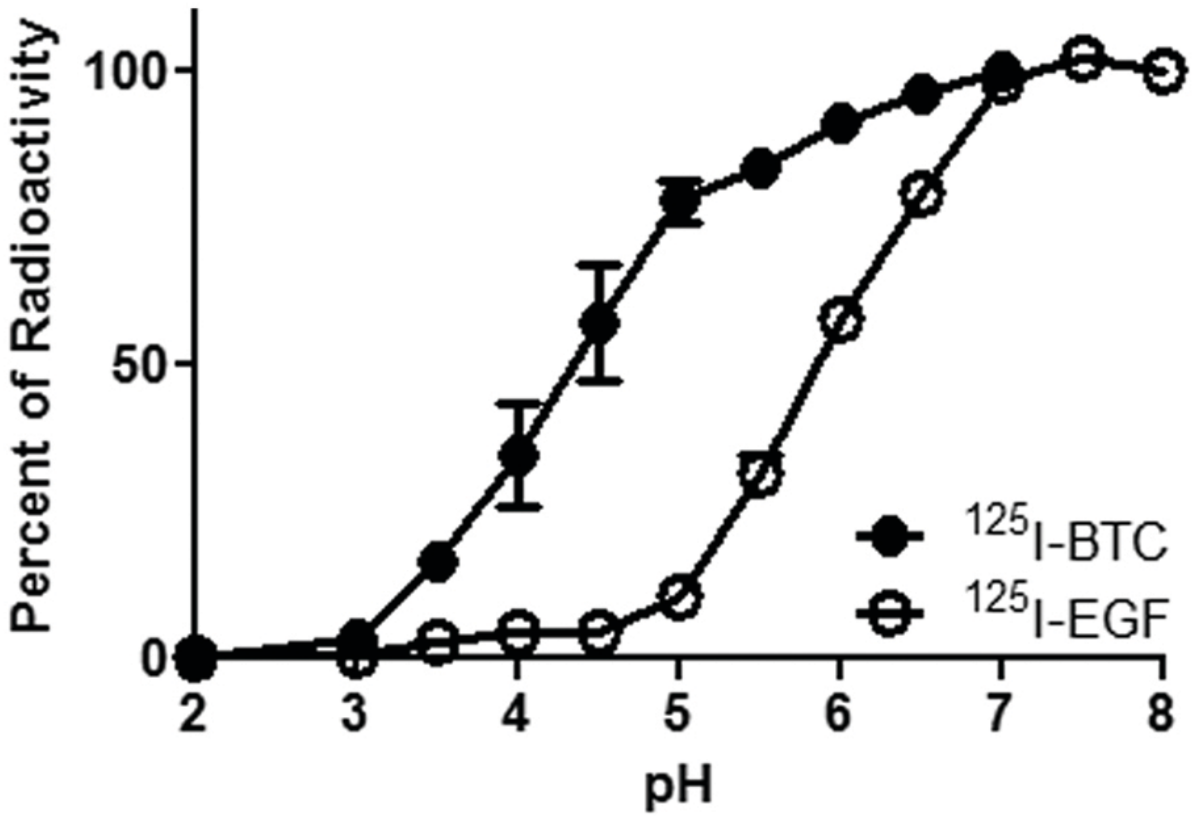

Figure 3 Rush et. al

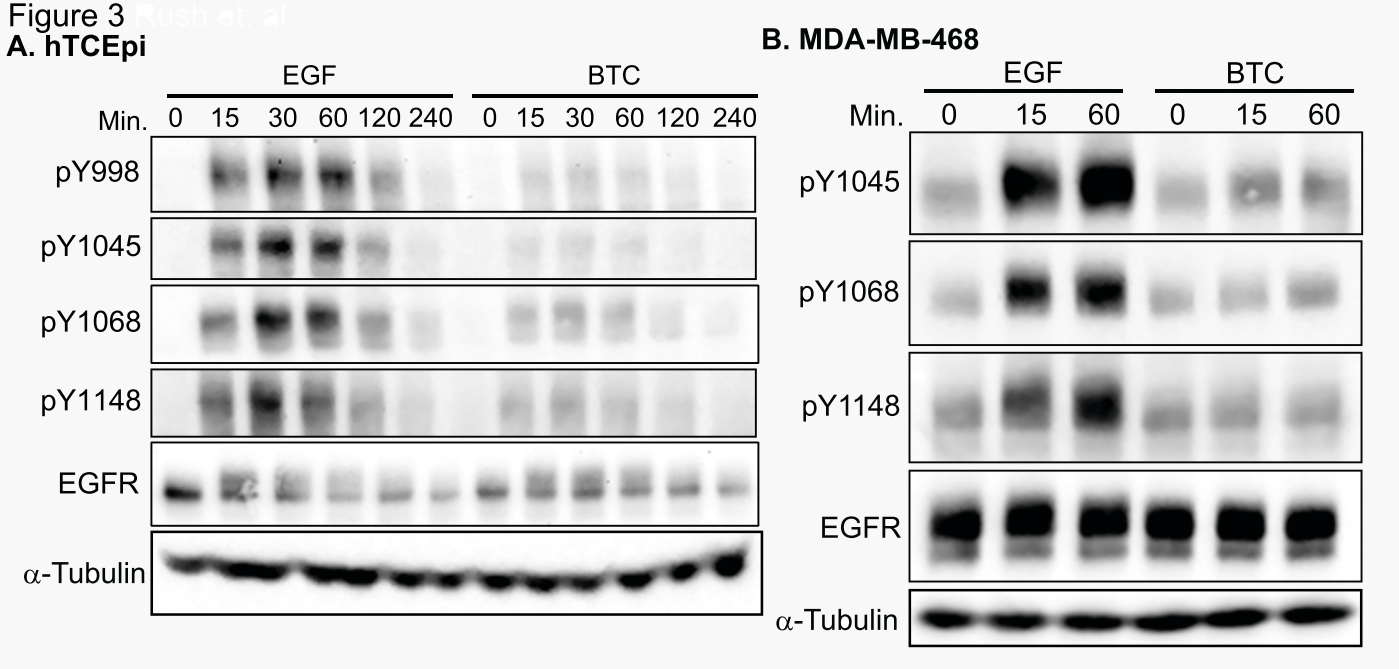

Figure 4

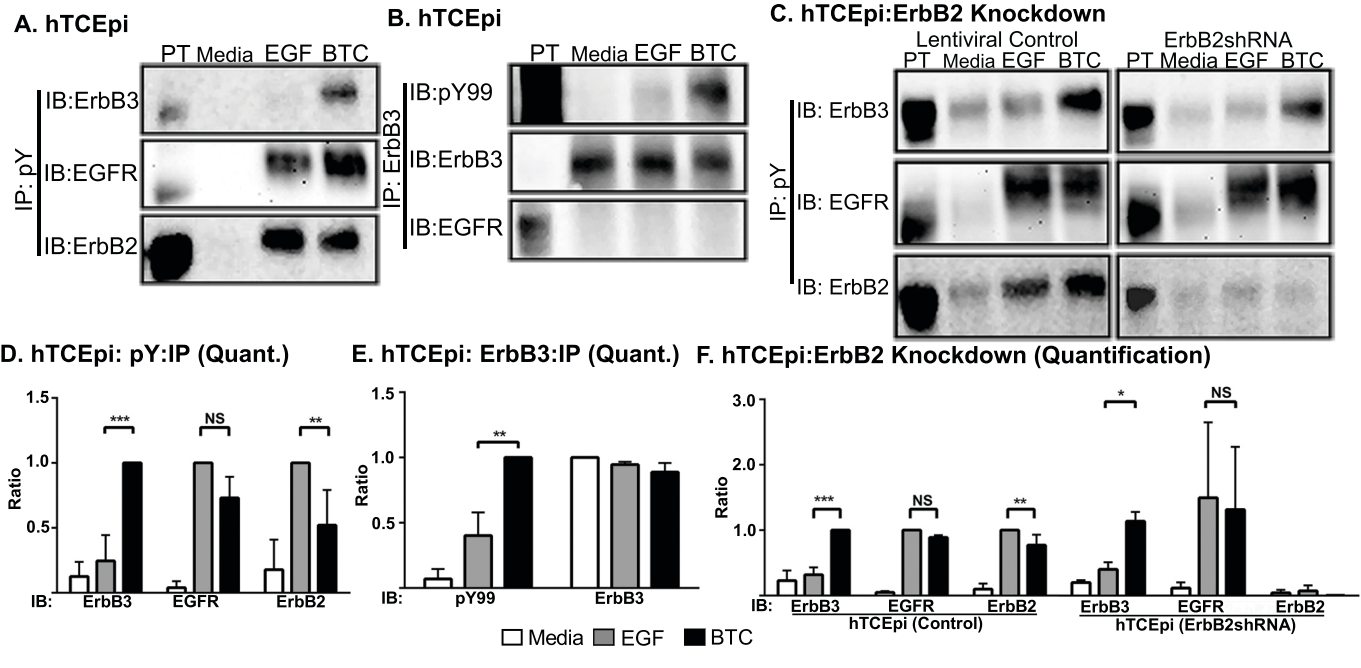
A. hTCEpi
PT Media EGF BTC
IP: pY
IB:ErbB3
IB:EGFR
IB:ErbB2
B. hTCEpi
PT Media EGF BTC
IP: ErbB3
IB:pY99
IB:ErbB3
IB:EGFR
C. hTCEpi:ErbB2 Knockdown
Lentiviral Control
ErbB2shRNA
PT Media EGF BTC
IP: pY
IB: ErbB3
IB: EGFR
IB: ErbB2
D. hTCEpi: pY:IP (Quant.)
Ratio
IB: ErbB3 EGFR ErbB2
E. hTCEpi: ErbB3:IP (Quant.)
Ratio
IB: pY99 ErbB3
F. hTCEpi:ErbB2 Knockdown (Quantification)
Ratio
IB: ErbB3 EGFR ErbB2 ErbB3 EGFR ErbB2
hTCEpi (Control)
hTCEpi (ErbB2shRNA)
Media EGF BTC

Figure 5

A. PLA: EGFR:ErbB3 Heterodimers

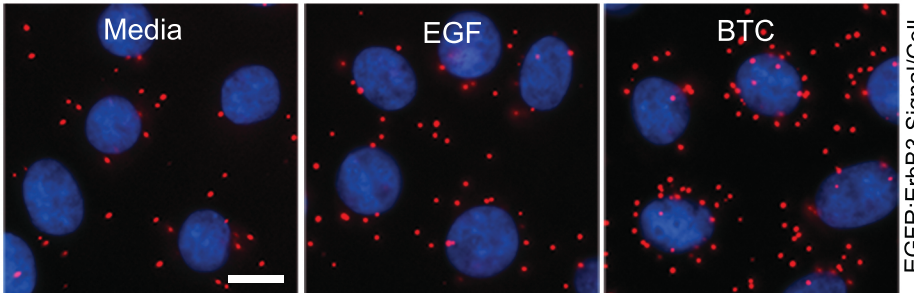

B. PLA: EGFR:ErbB3 (Total)

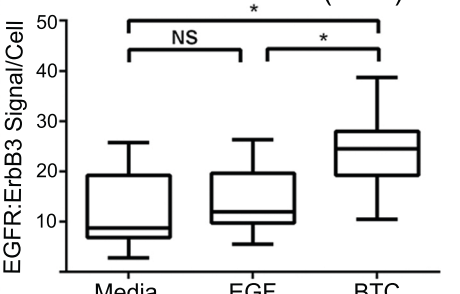

Figure 6